Statistica Sinica Preprint No: SS-13-106wR2	
Title	Statistical prediction of global sea level from global temperature
Manuscript ID	SS-13-222wR3
URL	http://www.stat.sinica.edu.tw/statistica/
DOI	10.5705/ss.2013.222w
Complete List of Authors	Peter Guttorp Alex Januzzi Daniel Jones Marie Novak Harry Podschwit Lee Richardson Aila S¨arkk¨a Colin Sowder and Aaron Zimmerman
Corresponding Author	Peter Guttorp
E-mail	peter@stat.washington.edu
Notice: Accepted version subject to English editing.	

STATISTICAL PREDICTION OF GLOBAL SEA LEVEL FROM GLOBAL TEMPERATURE

David Bolin, Peter Guttorp, Alex Januzzi, Daniel Jones,
Marie Novak, Harry Podschwit, Lee Richardson, Aila Särkkä,
Colin Sowder and Aaron Zimmerman

University of Washington, Norwegian Computing Center
and Chalmers University of Technology/University of Gothenburg

Abstract: Sea level rise is a threat to many coastal communities, and projection of future sea level for different climate change scenarios is an important societal task. In this paper, we first construct a time series regression model to predict global sea level from global temperature. The model is fitted to two sea level data sets (with and without corrections for reservoir storage of water) and three temperature data sets. The effect of smoothing before regression is also studied. Finally, we apply a novel methodology to develop confidence bands for the projected sea level, simultaneously for 2000-2100, under different scenarios, using temperature projections from the latest climate modeling experiment. The main finding is that different methods for sea level projection, which appear to disagree, have confidence intervals that overlap, when taking into account the different sources of variability in the analyses.

Key words and phrases: Singular spectrum smoothing, ARMA time series models, climate projections.

1. Introduction

One of the anticipated consequences of a warming climate is sea level rise. It is the result of two main processes: thermal expansion of sea water, and increased melting of glaciers and other land ice masses. However, the detailed understanding of the melting process of the Greenland and Antarctica ice sheets is still limited, and the uncertainties associated with these processes and with the role of the virtually unknown deep ocean are still very high (Stocker et al., 2010).

Partly because of these uncertainties, and since only very few climate models explicitly calculate sea level projections, some statistical approaches have been

developed to relate historic sea levels to temperatures (see Rahmstorf et al. (2011) for an overview). The thought is that such relations can be used to estimate sea level from climate model temperature projections (the term projections is used in climate modeling to denote simulations of future climate using specified forcings of the climate system). Since most climate models anticipate substantial warming in the 21st century under all scenarios considered, this means that the statistical models will be applied to a region of temperatures and sea levels outside the range of the training data. Generally, the statistical models have yielded estimated sea level rises that are substantially higher than the projections made by the climate models, fueling a concern that the climate model projections are too optimistic and that the climate models are missing crucial aspects of the physics causing sea level rise.

The motivation for this study is to produce statistically based global sea level projections with statistically defensible measures of uncertainty. Such projections, with uncertainty quantifications, are important tools for planners, decision-makers, and risk analysts dealing with issues of flooding, storm surges, and infrastructure in flood-prone areas. The uncertainty in future projections is typically visualized using point-wise confidence bands. These are calculated separately for each future time point t, and are constructed so that, with probability $1-\alpha$, the process is inside the confidence interval at time t. The problem with this approach is that the joint interpretation of the resulting confidence band is not what one might expect. If the point-wise confidence intervals have coverage probability $1-\alpha$, the probability for the process staying inside the confidence band *at all* time points considered in the future is in general much lower than $1-\alpha$. Even though this may be obvious to a trained statistician, planners and decision-makers may incorrectly interpret the confidence band as a simultaneous one, and thereby under-estimate the uncertainty in the projection. A better way to visualize the uncertainty is therefore to construct the confidence band jointly, so that it has the correct simultaneous interpretation: with probability $1-\alpha$, the process stays inside the confidence band at all time points for which future projections are made. The method for doing this is presented in Section 5.2. These simultaneous bands allow construction of confidence intervals for a given year by slicing vertically, and for a given sea level by slicing horizontally.

In section 2 we describe the main data sets and fit a statistical model to them. We compare our fit to a popular smoothing approach from the climate literature in section 3, and assess the forecast quality of the two models. Section 4 deals with the sensitivity to different data sets and data corrections. In section 5 we apply our statistical model to project global sea level, when the temperatures are given by the latest temperature projections developed for the recent Fifth Assessment Report (AR5) of the Intergovernmental Panel on Climate Change (IPCC) (Stocker et al., 2013). We calculate simultaneous confidence intervals for the sea level rise projections, which to our knowledge has not been done before. In section 6 we discuss our findings and compare them to the outcomes presented in AR5. All analyses in this paper are made using the R statistical package (R Core Team, 2013), and the code and data sets used are all available at `http://www.statmos.washington.edu/datacode.html`.

2. A statistical model relating sea level to temperature

Let T_t be the estimated annual mean global temperature at time t from the latest mean annual global temperature product from the Goddard Institute of Space Sciences (GISS) (Hansen et al., 2010), and H_t the corresponding annual mean global sea level (from Church and White (2011)). The temperature data goes up to the present, while the sea level data goes through 2009. Panel (a) in Figure 2.1 shows the scatter plot of the two time series with a fitted least squares line, using data from 1880–1999 (we are reserving the data from 2000–2009 for forecast verification).

Looking at the residual plot (panel (b) of Figure 2.1) it is clear that there is some temporal dependence present. Hence, we fit a time series regression model to the data, namely

$$H_t = \alpha + \beta T_t + \epsilon_t, \tag{2.1}$$

where ϵ_t is an integrated moving-average error structure, ARIMA(0,1,2), with drift but a non-significant regression coefficient. The choice of time series model is made using Akaike's Information Criterion (AIC) (Akaike, 1974) in the R package `forecast` (Hyndman et al., 2013). From a predictive point of view, this means that we would predict sea level not from temperature but from time. In order to get a more meaningful relationship, we therefore undo the integrated part of the model by fitting a time series regression model to the sea level differences

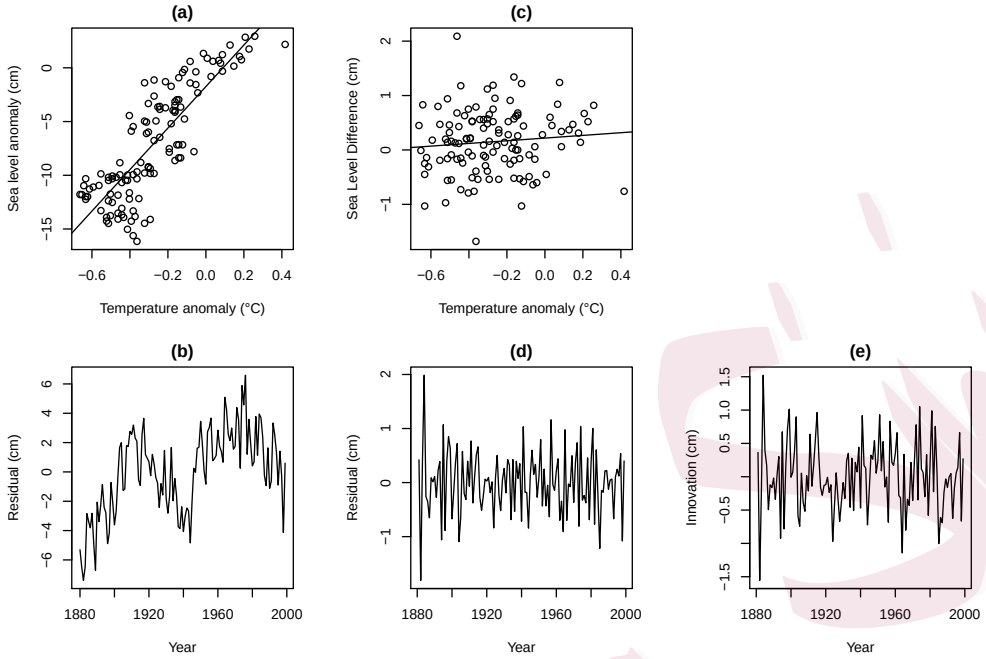

Figure 2.1: The Hansen et al. (2010) series of global temperatures plotted against the Church and White (2011) series of global sea levels (panel (a)) for the years 1880–1999 (relative to the years 1970–1999), with the fitted least squares regression line. The residual plot from the least squares regression (panel (b)) shows considerable temporal structure, leading us to fit temperature against differenced sea level (panel (c)). The residuals from the fitted line are shown in panel (d). They still show temporal structure, which has been removed in the estimated innovations from the time series fit in equation (2.2) (panel (e)).

ΔH_t, again using temperature T_t as a regressor, i.e.,

$$\Delta H_t = \gamma + \delta T_t + \eta_t, \tag{2.2}$$

where now η_t is a moving-average error structure of order 2. This fit is shown in panel (c) of Figure 2.1. The fitted moving average coefficients are -0.49 (standard error 0.08) and -0.24 (0.10), while the intercept γ is estimated to be 0.20 (0.02) and the slope δ is 0.16 (0.07), now significantly different from zero. Panel (e) of Figure 2.1 shows the estimated innovations from this fit, which pass a series of white noise tests, including autoregressive fitting, spectral estimation, and the white noise test of Lobato and Velasco (2004) with a P-value of 0.64.

The climate literature contains some papers where the type of analysis performed in this section is carried out using somewhat different techniques from ours. They are all based on the basic premise that the rate of sea level change should be related to temperature. Rahmstorf (2007) and Grinsted et al. (2009) both essentially use equation (2.2), while Vermeer and Rahmstorf (2009) add a regression term corresponding to temperature change, and Jevrejeva et al. (2009) replace the temperature by the radiative forcing. Our analysis indicates that the additional term in Vermeer and Rahmstorf (2009) is not significantly different from zero when taking the time series structure into account. Furthermore, the response of the climate to radiative forcing is linear in temperature (Shine, 2000) to first order, so the empirical models using temperature or radiative forcing are very similar. On the other hand, when trying to project future sea levels they are very different. A projection using the relationship between sea level and radiative forcing looks similar to the scenarios (which prescribe forcings, see section 5). A projection that uses the climate model output for temperature, which is influenced by internal climate processes in addition to the forcing prescribed by the scenarios, does not follow the scenarios, since the climate system reaction to forcings is not immediate. In fact, even if the greenhouse gas emissions decrease, the concentration in the atmosphere will stay high for a long time, so the projections relating sea level to radiative forcing are not very believable from a physical point of view. For conciseness, we will in the next section focus on comparing our analysis to that of Rahmstorf (2007).

3. The effect of smoothing

In order to relate the change in sea level to temperature, Rahmstorf (2007) first smoothed both series, obtaining $\tilde{T}_t$ and $\tilde{H}$, respectively. The smoother used was a singular spectrum analysis (SSA) decomposition (Vautard and Yiou, 1992) with a 15-year window. His regression equation was

$$d\tilde{H}_t/dt = a(\tilde{T}_t - T_0) + \epsilon_t \tag{3.1}$$

where T_0 corresponds to an equilibrium temperature and ϵ_t are errors. The rate $d\tilde{H}_t/dt$ was approximated by differencing $\tilde{H}$. Rahmstorf did not assume that the errors are independent. Rather, he binned the data in five-year bins, and performed ordinary least squares estimation of the parameters a and T_0. The equations (2.2) and (3.1), apart from the effect of smoothing, can be related to

each other by setting $a = \gamma$ and $T_0 = -\delta/\gamma$. The estimates (in terms of the parametrization in equation (2.2) and using the data from the previous section) are $\tilde{\gamma} = 0.19$ (0.01) and $\tilde{\delta} = 0.16$ (0.03), where the tilde corresponds to smoothed estimates, and we use a time series regression model with ARMA(2,1)-structure, again chosen by AIC. The estimates from the smoothed and raw analyses are not significantly different. However, the estimated innovations from the smoothed fit do not pass the white noise test (P-value 0.027). Data, residuals and estimated innovations are shown in Figure 2 of the Supplementary material.

The SSA smoother is not one commonly used in statistics. It was introduced in paleoclimatology (Vautard and Ghil, 1989) to handle noisy data, particularly when numerical derivatives are needed. The smoothing parameter chosen by Rahmstorf (2007) maximizes the correlation in the model (3.1). The implementation of the SSA smoother used here first extends the data using local linear regression by a window's worth of data on either side of the data set before smoothing, in order to diminish the edge effects.

A difficulty with using smoothed data in regression is that the residuals will tend to have a more complicated time series structure (see section 4). At the same time, the correlation between the two series in the regression increases, but this correlation is spurious and induced by the smoothing.

We assess the quality of the model fits by forecasting the values for the years 2000 through 2009, which were not used in the fitting. Figure 3.1 shows the forecasts and the reserved observations for the raw (left) and smoothed (right) models, respectively. In the unsmoothed (or raw) forecast, the reserved data fall inside the 90% prediction bands (we use 90% confidence levels since this is what is commonly used in the IPCC assessments), but for the smoothed forecast the first two values are too high.

4. Sensitivity analysis

The projections obtained from time series regression may depend on which sea level and temperature data are used. In this section we compare the results based on two sea level data sets and three temperature data sets. In addition, we study how the so-called reservoir correction (explained below) to observed sea level affects the results.

There are different products estimating global temperature (e.g. Hansen

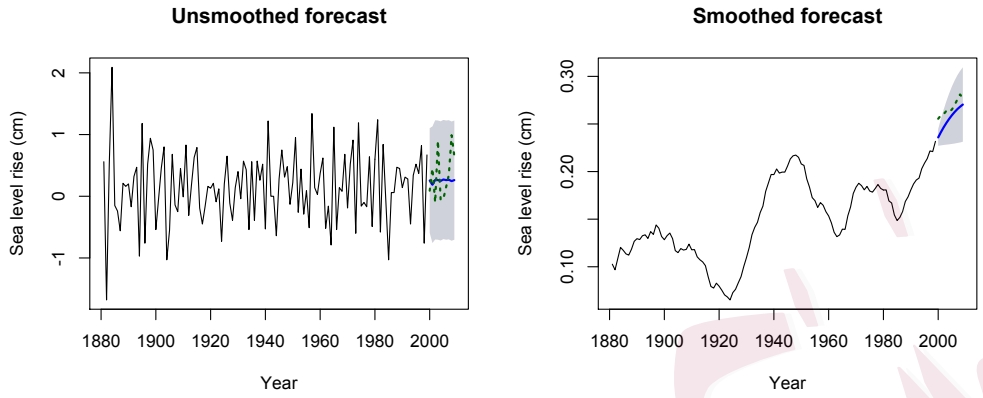

Figure 3.1: Forecast (solid), 90% forecast bands (grey) and reserved data (dotted) for our model given by equation (2.2) (left panel) and by Rahmstorf's model given by equation (3.1) (right panel). The reserved data fall in the forecast band for the raw differences (left) but not for the smoothed differences (right). The sea level rise series are shown in black.

et al. (2001); Morice et al. (2012)) from land station data, ship logs, buoy data etc. They are based on somewhat different (but largely overlapping) data sets. Estimation approaches range from local spatial methods to principal components. Likewise, there are different products describing global sea level (e.g. Church and White (2011); Nerem et al. (2010)). Here the sources are mainly tide gauges and bottom pressure gauges, and more recently satellite measurements as well. The sea level data have been adjusted for glacial rebound effects. In this section we look at the sensitivity of our analysis to the particular data set used.

The GISS global mean temperature data product used by Rahmstorf (2007) is an earlier version than that we used in section 2 above. The data sets for temperature as well as for sea level undergo continuing refinements. Often new stations (with historical data) are added to the network used in the analysis. Also, methods for correcting data (e.g., adjusting for relocation or replacement of a measurement instrument) are continually being revised. In addition to the GISS data used by Rahmstorf (2007), which we will denote R07 GISS, and our current GISS data set (downloaded in December 2013 and based both on a larger set of observations and a revised data correction approach), we will also consider a third

global mean temperature product, HadCRUT4 (also downloaded in December 2013), developed by the Hadley Centre of the UK Met Office (Morice et al., 2012). There is no obvious advantage of one data product over the other. In terms of sea level data, we compare using the older Church and White (2006) and the more recent Church et al. (2011) data products. The latter is an updated product which uses more stations.

We also consider the effect of using the land reservoir corrected series $\hat{H}_t$ proposed by Vermeer and Rahmstorf (2009), who applied a correction factor to sea level data before forming anomalies and smoothing:

$$\hat{H}_t = H_t + 1.65 + (3.7/\pi)\arctan((t - 1978)/13). \tag{4.1}$$

Chao et al. (2008) provided an in depth analysis of artificial reservoir water containment in response to the 2007 IPCC report (Solomon et al., 2007), which noted that the water balance equations for global sea level rise were not (at the time of the report) satisfactory, in part due to relatively unstudied contributions to the balance from land-based water alterations. After collecting information about all reasonably large reservoirs around the world, they modeled the amount of water that had been artificially withheld from the oceans. Using their results, they argued that the stored water, if allowed to run into the ocean, would further increase the sea level rise, and therefore should be accounted for when modeling global sea level. This is clearly important when considering Earth's water budget (Church et al., 2011), but seems less relevant to projections of actual sea level. Of concern to policy makers is the observed global sea level, not the global sea level with some anthropogenic drivers removed. Since these drivers tend to reduce sea level, correcting for them will produce a higher sea level than the observed global sea level. Two options are to try to predict these anthropogenic drivers into the future and correct for them, which requires a number of assumptions about future behavior, or to make the assumption that the empirical model will be robust to these drivers.

Later work by Wada et al. (2010) demonstrates that ground water depletion, which adds water *into* the ocean, has been occurring at generally higher rates compared to the reservoir correction and would actually balance and reverse the effects of the reservoir correction if included. Because of these results, we chose not to use a reservoir correction in our analysis in section 2. Below we illustrate

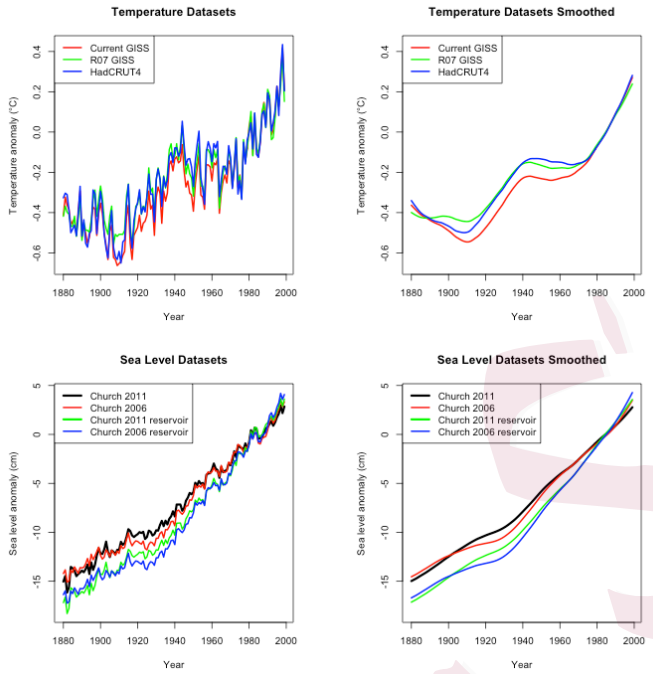

Figure 4.1: Comparing temperature datasets (top row) and sea level datasets (bottom row) for both the original data (left column) and the smoothed data (right column).

the effect of the reservoir correction as well as the effect of using different data sets in the analysis. We have not found any reference to how equation (4.1) was derived, and our uncertainty analyses therefore does not take into account the uncertainty in the reservoir correction.

Figure 4.1 shows the various data sets, and Tables 4.1 and 4.2 compare the model structure and fits of the raw and smoothed models to each of the combinations of data sets. The smoothed time series models always have a more complicated structure than the raw models. There is hardly any difference between using the current GISS data set and using the HadCRUT4 temperatures, while the older GISS data set (using fewer stations and different homogenization technique) yields higher slope estimates. The earlier sea level data set and the reservoir correction always yield higher slopes. The smoothed and raw analyses yield essentially the same parameter values, with the standard errors of the smoothed series smaller by a factor of 2-3.

Sea Level Data	Temperature Data	Raw	Smoothed
Church 2011	Current GISS	(0,0,2)	(2,0,1)
	R07 GISS	(0,0,2)	(6,0,3)
	HadCRUT4	(0,0,2)	(2,0,1)
Church 2006	Current GISS	(0,0,2)	(6,0,4)
	R07 GISS	(0,0,2)	(2,0,1)
	HadCRUT4	(1,0,1)	(2,0,1)
Church 2011 Res	Current GISS	(0,0,2)	(2,0,1)
	R07 GISS	(1,0,1)	(6,0,4)
	HadCRUT4	(1,0,1)	(2,0,1)
Church 2006 Res	Current GISS	(1,0,1)	(6,0,4)
	R07 GISS	(1,0,1)	(6,0,4)
	HadCRUT4	(0,0,2)	(6,0,4)

Table 4.1: ARIMA models for raw (unsmoothed) and SSA smoothed data. Res stands for reservoir correction.

5. Projecting Sea Level Rise

The models discussed so far can be applied to project global sea level using the latest temperature projections developed for the recent Fifth Assessment Report of the IPCC (AR5, Stocker and Dahe (2013)). First we explain how to project future climate events, e.g. global temperature, by using climate models, and then we present a novel approach to compute simultaneous confidence intervals for the projections.

Climate models (large deterministic models solving a system of partial differential equations describing the various aspects of the climate system) are used to project future climate events. Since there are no global models to predict the policy options available to politicians, and what decisions they will make, it is standard practice to develop some scenarios for the future, describing some possible policy outcomes. The current set of scenarios are called representative concentration pathways (RCPs)(Moss et al., 2010). The four RCPs used are each a representation of different combinations of variables that as a whole provide a plausible descriptive framework regarding how future climate may evolve. The variables involved in the four scenarios include socio-economic changes, changes in technology, changes in energy and land use, and changes in emissions of greenhouse gases and air pollutants. As a whole, the RCPs represent varying outcome

		Rawl		Smoothed		Raw		Smoothed	
Sea Level Data	Temperature Data	γ	SE	γ	SE	δ	SE	δ	SE
Church 2011	Current GISS	0.20	0.02	0.19	0.01	0.16	0.07	0.16	0.03
	R07 GISS	0.19	0.02	0.19	-	0.19	0.08	0.18	-
	HadCRUT4	0.19	0.02	0.19	0.01	0.17	0.07	0.17	0.03
Church 2006	Current GISS	0.24	0.03	0.24	0.02	0.31	0.10	0.33	0.06
	R07 GISS	0.23	0.03	0.23	0.02	0.36	0.11	0.36	0.06
	HadCRUT4	0.22	0.02	0.22	0.01	0.31	0.08	0.32	0.05
Church 2011 Res	Current GISS	0.25	0.03	0.24	0.01	0.27	0.07	0.25	0.04
	R07 GISS	0.25	0.02	0.23	0.02	0.31	0.07	0.27	0.05
	HadCRUT4	0.24	0.02	0.23	0.01	0.28	0.07	0.27	0.04
Church 2006 Res	Current GISS	0.29	0.03	0.28	0.02	0.40	0.07	0.39	0.05
	R07 GISS	0.28	0.02	0.27	0.02	0.46	0.09	0.44	0.05
	HadCRUT4	0.27	0.03	0.27	0.01	0.40	0.09	0.41	0.04

Table 4.2: Parameters and standard error for each model and data set combination. An entry "-" means that the fitting procedure failed to compute standard errors. Res stands for reservoir correction.

levels of radiative forcing, i.e., factors that cause a change in the net radiation received and emitted by Earth. RCPs are constructed to include representations from low, intermediate, and extreme scenarios of radiative forcing (van Vuuren et al., 2011). The four RCPs, labeled according to their predicted radiative forcing (W/m^2) in 2100, are RCP2.6, RCP4.5, RCP6.0, and RCP8.5. For example, RCP 2.6 corresponds to implementing serious reductions in greenhouse gas emissions worldwide leading to a decline in radiative forcing starting around 2050, while RCP 8.5 allows a continuing increase in these emissions. This structure allows the RCPs to describe a wide range of uncertainty. With the variables combined, each individual RCP provides a basis for assessing mitigation options, associated costs, and potential future impacts on climate with the goal of informing policy-making.

In this section we first describe briefly the experiment from which our climate projections are obtained, and then how for each of the four RCPs we can use our model to develop uncertainty bands for sea level rise, taking account both of the variability between models and of the uncertainty in the fitted relationship between global sea level and global temperature.

5.1 The CMIP5 Experiment

In order to make projections comparable for the different RCPs, we have selected those climate models from the Coupled Model Intercomparison Project

(1) bcc-csm1-1, China	(2) CCSM4, USA
(3) CESM1-CAM5, USA	(4) CSIRO-Mk3-6-0, Australia
(5) FGOALS-s2, China	(6) FIO-ESM, China
(7) GFDL-CM3, USA	(8) GFDL-ESM2G, USA
(9) GFDL-ESM2M, USA	(10) GISS-E2-R30, USA
(11) HadGEM2-AO, UK	(12) IPSL-CM5A-LR, France
(13) MIROC5, Switzerland	(14) MIROC-ESM, Switzerland
(15) MIROC-ESM-CHEM, Switzerland	(16) MRI-CGCM3, Japan
(17) NorESM1-M, Norway	(18) NorESM1-ME, Norway

Table 5.1: Climate models used.

Phase 5 (CMIP5) experiment (Taylor et al., 2012) with global mean temperature computations for all the four RCPs for the years 2000-2100; a total of 18 models out of 45 for which we have data. These 18 models span the full range of model output for each of the scenarios. The CMIP5 experiment, which consists of comparable runs from nearly all the world's serious climate system models, formed part of the basis for the most recent IPCC assessment (Stocker et al., 2013). Table 5.1 shows which climate models we are using (for URLs to more information about each of these models, see `http://courses.washington.edu/statclim/GCMs_used.html`).

Figure 5.1 shows the temperature projections for the 18 models (each model has a separate color in the online version) for the four different RCPs. The range of temperatures gives a rough idea of the model uncertainty. While all the models solve the same set of partial differential equations to describe the atmosphere, they vary in the way they numerically solve them, how they include other parts of the climate system, how they parametrize processes that occur on smaller scales than the grids used in the numerical solution, etc. The rates of temperature increase varies with the RCP, and the different models do not respond identically to a given scenario.

It is worth noting that some modeling groups have more than one model in this selection. Commonly such models have some code in common, and assuming that these models are independent or exchangeable, and that the union of them constitute an estimate of the between-model variability, is an oversimplification (Jun et al., 2008). This variability is undoubtedly an underestimate, but it is not

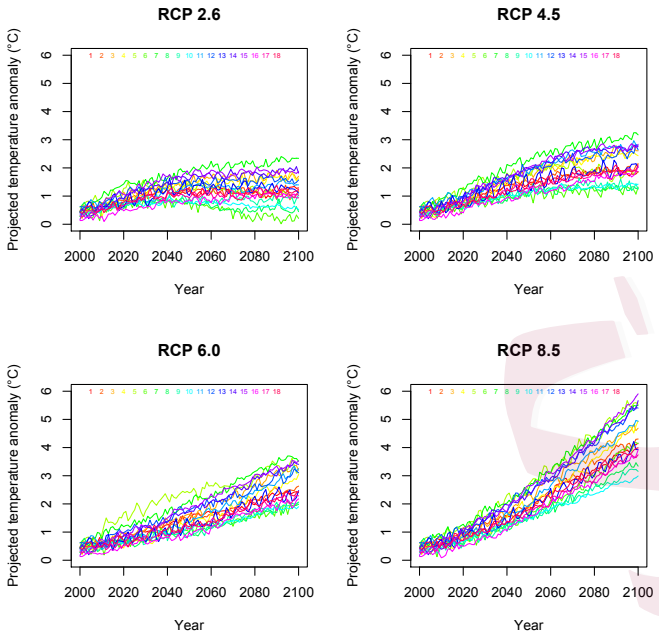

Figure 5.1: Climate model projections of 21st century global mean temperatures for the four RCPs. Each model has the same color in each panel. The numbers are colored as the corresponding path, and refer to Table 5.1. The response to the different forcing scenarios is different between models.

easy to correct for it. However, the spread in these temperature projections yields a better uncertainty quantification than the common approach to average all the projections. As in standard regression methods, we condition on the covariate values, namely the different global temperature projections.

5.2 Constructing Confidence Intervals for Projected Sea Level Rise

Recall that we, in order to visualize the uncertainty in the future projections, want to construct a simultaneous confidence band so that with probability $1-\alpha$, the process stays inside the confidence band at all time points that are shown in the future projection. To do this, we need the joint predictive distribution for the process at all predicted time points. The predictive distribution for the global sea level $\mathbf{H} = \{H_{t_1}, \ldots, H_{t_2}\}$ in a future period $t \in [t_1, t_2]$, conditionally on one climate model output, the past sea levels and temperatures, and the estimated

model parameters, is Gaussian with mean value $\mu = \mu_p - \mathbf{\Sigma}_{op}\mathbf{\Sigma}_o^{-1}(\mathbf{x}_o - \mu_o)$, and covariance matrix $\mathbf{\Sigma} = \mathbf{\Sigma}_p - \mathbf{\Sigma}_o^{-1}\mathbf{\Sigma}_{op}^T$. Here μ_o and $\mathbf{\Sigma}_o$ denote the mean and covariance for the observed sea level, μ_p and $\mathbf{\Sigma}_p$ denote the mean and covariance for the sea level at the prediction time points, and $\mathbf{\Sigma}_{op}$ is the cross covariance matrix between the observed and predicted sea levels. All these quantities are given by the model (2.2), or, in terms of sea level rather than sea level rise,

$$H_t = \int_{t_0}^{t} (\gamma + \delta T_u)du + \zeta_t, \tag{5.1}$$

where ζ_t are the accumulated innovations. In order to take the uncertainty in the climate model outputs into account, we also integrate the predictions over all available climate model outputs. Giving the $K = 18$ climate projections equal weights yields the final predictive distribution as a mixture of Gaussian distributions,

$$\pi(\mathbf{H}) = \sum_{k=1}^{K} \frac{1}{K(2\pi)^{t_p/2}|\mathbf{\Sigma}|^{1/2}} \exp\left(-\frac{1}{2}(\mathbf{H} - \mu_k)^\intercal \mathbf{\Sigma}^{-1}(\mathbf{H} - \mu_k)\right), \tag{5.2}$$

where t_p is the number of prediction time points and μ_k is the mean for the predictive distribution based on climate model k.

A point-wise confidence band is given by $[q_{\alpha/2}(t), q_{1-\alpha/2}(t)]$, where $q_\alpha(t)$ denotes the α-quantile in the marginal distribution $\pi(H_t)$. Since we have analytic expressions for the marginal distributions, it is computationally easy to find these quantiles using numerical optimization.

A simultaneous confidence band, such that the sea level with probability $1-\alpha$ stays inside the band at all times $t \in [t_1, t_2]$ can be constructed by considering the joint distribution for $\mathbf{H}$. We construct this simultaneous confidence band by finding the value of ρ such that

$$\mathbf{P}(q_\rho(t) < H_t < q_{1-\rho}(t), t_1 < t < t_2) = 1 - \alpha. \tag{5.3}$$

Finding ρ requires that we can calculate joint probabilities of this type efficiently, which is not as easy as finding the marginal quantiles. This can be done using the sequential integration method in Bolin and Lindgren (2014), which is implemented in the R package `excursions` (see Supplemental material for more details). The method can easily be applied in a Bayesian framework as well, although we are not doing that here.

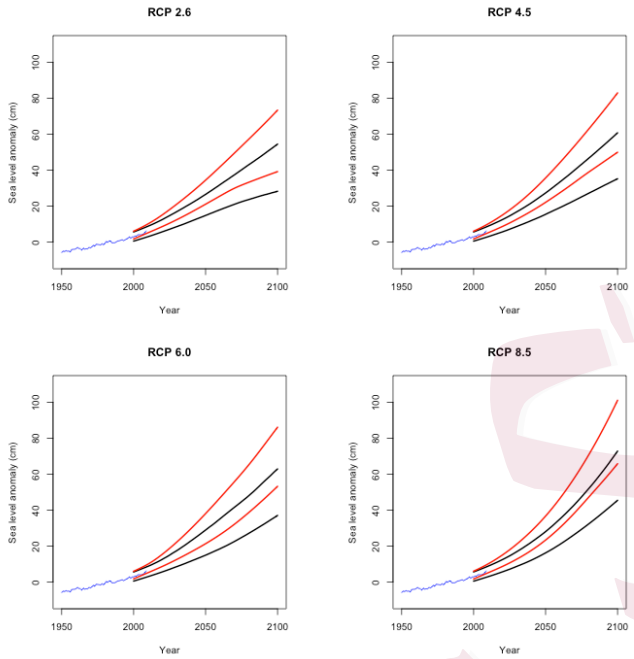

Figure 5.2: 90% sea level projection simultaneous confidence sets for 2000-2100 for four climate scenarios using raw (dark) and smoothed (light) projections, where the smoothed projections employ the reservoir correction. The sea level data end at 2009.

Applying the reservoir correction of Vermeer and Rahmstorf (2009) yields higher values than the raw projections (Figure 5.2). However, the projection uncertainty bands overlap, indicating that the projection uncertainty is such that we cannot statistically distinguish models with and without reservoir corrections. When comparing raw and smoothed projections without the reservoir correction (not shown) there is very little difference between the two uncertainty bands.

6. Discussion

IPCC's AR5 (Stocker et al., 2013) looked at global sea level rise in the climate models from the CMIP5 (Taylor et al., 2012) experiment. The report is not completely clear as to how the sea levels were obtained, as only very few models actually calculate sea level over geode. Table 6.1 gives the median projection and 90% pointwise confidence intervals for sea level rises in 2100 relative to the mean sea level from 1970-1999 for the smoothed data with reservoir correction,

	RCP2.6		RCP4.5		RCP6.0		RCP8.5	
Model	Med	Set	Med	Set	Med	Set	Med	Set
Raw	40	32-50	46	38-56	46	40-59	58	48-70
Reservoir	55	42-70	63	52-80	64	55-84	81	68-99
AR5	44	26-58	56	33-68	58	35-70	76	51-95

Table 6.1: Point estimates (medians; Med in the table heading) and 90% point-wise confidence sets (Set in the table heading) for sea level rise (cm) projected in 2100 for the four climate scenarios used in AR5. We show our analysis using the raw data (row label Raw), the smoothed data with reservoir correction (row label Reservoir), and the AR5 model results (row label AR5). All numbers are relative to the 1970-1999 mean sea level.

for our unsmoothed analysis, along with AR5 projected rises (the latter are given relative to 1986-2005 in the assessment report, but have here been adjusted to the same reference period as our analyses).

The indication here is that the statistical fit to historical data without reservoir correction yields slightly lower sea level rise than the rise projected in the climate models, while the projections from the smoothed model with reservoir corrections are somewhat higher. The uncertainty intervals for the 2100 projections are similar in size, with the exception that the raw projection for the high scenario RCP8.5 are somewhat narrower than the other two. All the intervals overlap, showing some consistency in the uncertainty assessments.

If there are sources of sea level rise, such as substantial land ice melt, and the gravitational changes resulting from that (Mitrovica et al., 2009), which have not been observed in the historical data, the empirical model cannot account for such changes, but neither are these very well represented by current climate models (Stocker et al., 2013, Ch. 13).

Acknowledgment

We are very grateful to Claudia Tebaldi who provided the data needed to fit the model in Vermeer and Rahmstorf (2009) and patiently answered all our questions. We acknowledge the World Climate Research Programme's Working Group on Coupled Modelling, which is responsible for CMIP, and we thank the climate modeling groups (listed in Table 5.1 of this paper) for producing and making available their model output. The global temperature products

were obtained from the Goddard Institute for Space Sciences web pages and the Hadley Center web pages, while the global sea level product came from the CSIRO sea level web pages. The project had partial support from the NSF Research Network on Statistics in the Atmosphere and Ocean Sciences (STATMOS) through grant DMS-1106862 and by the Knut and Alice Wallenberg Foundation. This research was done as a project in a course in statistical climatology, in which the authors participated. Further material can be found at `http://courses.washington.edu/statclim`. Comments from referees and co-editors of this volume have improved the presentation of our findings.

References

Akaike, H. (1974). A new look at the statistical model identification. *IEEE Transactions on Automatic Control 19*, 716–723.

Bolin, D. and F. Lindgren (2014). Excursion and contour uncertainty regions for latent Gaussian models (in press). *Journal of the Royal Statistical Society Series B*.

Chao, B. F., Y. Wu, and Y. Li (2008). Impact of artificial reservoir water impoundment on global sea level. *Science 320*(5873), 212–214.

Church, J. and N. White (2006). A 20th century acceleration in global sea-level rise. *Geophysical Research Letters 33*, doi:10.1029/2005GL02482.

Church, J. and N. White (2011). Sea-level rise from the late 19th to the early 21st century. *Surveys in Geophysics 32*, 585–602.

Church, J., N. White, L. Konikow, C. Domingues, J. Cogley, E. Rignot, J. Gregory, M. van den Broeke, A. Monaghan, and I. Velicogna (2011). Revisiting the earth's sea-level and energy budgets from 1961 to 2008. *Geophysical Research Letters 38*(18), doi:10.1029/2011GL048794.

Grinsted, A., J. Moore, and S. Jevrejeva (2009). Reconstructing sea level from

paleo and projected temperatures 200 to 2100 ad. *Climate Dynamics 34*, 461–472.

Hansen, J., R. Rued, M. Sato, M. Imhoff, W. Lawrence, D. Easterling, T. Peterson, and T. Karl (2001). A closer look at United States and global surface temperature change. *J. Geophys. Res. 106*, 23947–23963.

Hansen, J., R. Ruedy, M. Sato, and K. Lo (2010). Global surface temperature change. *Rev. Geophys. 48*, doi:10.1029/2010RG000345.

Hyndman, R. J., G. Athanasopoulos, S. Razbash, D. Schmidt, Z. Zhou, Y. Khan, and C. Bergmeir (2013). *forecast: Forecasting functions for time series and linear models*. R package version 4.8.

Jevrejeva, S., A. Grinsted, and J. Moore (2009). Anthropogenic forcing dominates sea level rise since 1850. *Geophysical Research Letters 36*, L20706.

Jun, M., R. Knutti, and D. Nychka (2008). Spatial analysis to quantify numerical model bias and dependence: How many climate models are there? *Journal of the American Statistical Association 103*, 934–947.

Lobato, I. and C. Velasco (2004). A simple and general test for white noise. Technical Report 112, Econometric Society Latin-America Meetings.

Mitrovica, J. X., N. Gomez, and P. U. Clark (2009). The sea-level fingerprint of west antarctic collapse. *Science 323*, 753.

Morice, C. P., J. J. Kennedy, N. A. Rayner, and P. D. Jones (2012). Quantifying uncertainties in global and regional temperature change using an ensemble of observational estimates: The hadcrut4 dataset. *J. Geophys. Res. 117*, D08101.

Moss, R. H., J. A. Edmonds, K. A. Hibbard, M. R. Manning, S. K. Rose, D. P. van Vuuren, T. R. Carter, S. Emori, M. Kainuma, T. Kram, G. A. Meehl, J. F. B. Mitchell, N. Nakicenovic, K. Riahi, S. J. Smith, R. J. Stouffer, A. M. Thomson, J. P. Weyant, and T. J. Wilbanks (2010). The next generation of scenarios for climate change research and assessment. *Nature 463*, 747–756.

Nerem, R. S., D. Chambers, C. Choe, and G. T. Mitchum (2010). Estimating mean sea level change from the TOPEX and Jason altimeter missions. *Marine Geodesy 33*, 435.

R Core Team (2013). *R: A Language and Environment for Statistical Computing*. Vienna, Austria: R Foundation for Statistical Computing.

Rahmstorf, S. (2007). A semi-empirical approach to projecting future sea-level rise. *Science 315*, 368–370.

Rahmstorf, S., M. Perrette, and M. Vermeer (2011). Testing the robustness of semi-empirical sea level projections. climate dynamics. *Climate Dynamics 39*, 861–875.

Shine, K. P. (2000). Radiative forcing of climate change. *Space Science Reviews 94*, 363–373.

Solomon, S., D. Qin, M. Manning, Z. Chen, M. Marquis, K. Averyt, M. Tignor, and H. Miller (2007). *Contribution of Working Group I to the Fourth Assessment Report of the Intergovernmental Panel on Climate Change*. Cambridge University Press.

Stocker, T., Q. Dahe, G.-K. Plattner, M. Tignor, S. Allen, and P. Midgley (2010). *IPCC Workshop on Sea Level Rise and Ice Sheet Instabilities*. IPCC Working Group I Technical Support Unit.

Stocker, T., D. Qin, G.-K. Plattner, M. Tignor, S. K. Allen, J. Boschung, A. Nauels, Y. Xia, V. Bex, and P. Midgley (2013). *Climate Change 2013: The Physical Science Basis. Contribution of Working Group I to the IPCC Fifth Assessment Report of the Iintergovernmental Pabel on Climate Chang*. Cambridge University Press.

Taylor, K., R. Stouffer, and G. Meehl (2012). An overview of CMIP5 and the experiment design. *Bull. Amer. Meteor. Soc. 93*, 485–498.

van Vuuren, D. P., J. Edmonds, M. Kainuma, K. Riahi, A. Thomson, K. Hibbard, G. C. Hurtt, T. Kram, V. Krey, J.-F. Lamarque, T. Masui, M. Meinshausen, N. Nakicenovic, S. J. Smith, and S. K. Rose (2011). The representative concentration pathways: an overview. *Climatic Change 109*, 5–31.

Vautard, R. and M. Ghil (1989). Singular spectrum analysis in nonlinear dynamics, with applications to paleoclimatic time series. *Physica D: Nonlinear Phenomena 35*, 395–424.

Vautard, R. and M. Yiou, P. Ghil (1992). Singular-spectrum analysis: a toolkit for short, noisy chaotic signals. *Physica D: Nonlinear Phenomena 58*, 95–126.

Vermeer, M. and S. Rahmstorf (2009). Global sea level linked to global temperature. *Proceedings of the National Academy of Sciences 106*, 21527–21532.

Wada, Y., L. P. van Beek, C. M. van Kempen, J. W. Reckman, S. Vasak, and M. F. Bierkens (2010). Global depletion of groundwater resources. *Geophysical Research Letters 37*(20), doi:10.1029/2010GL044571.

Chalmers University of Technology and the University of Gothenburg
E-mail: davidbolin@gmail.com
University of Washington and Norwegian Computing Center
E-mail: peter@stat.washington.edu
University of Washington
E-mail: ajanuzzi@uw.edu
University of Washington
E-mail: danjones0806@gmail.com
University of Washington
E-mail: menovak@uw.edu
University of Washington
E-mail: hpodschwit@gmail.com
University of Washington
E-mail: leerichardson2013@gmail.com
Chalmers University of Technology and the University of Gothenburg
E-mail: aila@chalmers.se
University of Washington
E-mail: csowder@uw.edu
University of Washington
E-mail: azimmer@uw.edu